

**ORIGINAL ARTICLE**

# UVB-induced depletion of donor-derived dendritic cells prevents allograft rejection of immune-privileged hair follicles in humanized mice

Jin Yong Kim<sup>1,2,3</sup>  | Bo Mi Kang<sup>1,2,3</sup> | Ji Su Lee<sup>1,2,3</sup> | Hi-Jung Park<sup>4,5</sup> |  
Hae Joo Wi<sup>4,5</sup> | Ji-Seon Yoon<sup>2,3</sup> | Curie Ahn<sup>4,6</sup> | Sue Shin<sup>7,8,9</sup> | Kyu Han Kim<sup>1,2,3</sup> |  
Kyeong Cheon Jung<sup>4,5</sup> | Ohsang Kwon<sup>1,2,3</sup> 

<sup>1</sup>Department of Dermatology, Seoul National University College of Medicine, Seoul, Korea

<sup>2</sup>Institute of Human-Environment Interface Biology, Medical Research Center, Seoul National University, Seoul, Korea

<sup>3</sup>Laboratory of Cutaneous Aging and Hair Research, Biomedical Research Institute, Seoul National University Hospital, Seoul, Korea

<sup>4</sup>Transplantation Research Institute, Medical Research Center, Seoul National University College of Medicine, Seoul, Korea

<sup>5</sup>Department of Pathology and Graduate Course of Translational Medicine, Seoul National University College of Medicine, Seoul, Korea

<sup>6</sup>Department of Internal Medicine, Seoul National University College of Medicine; Transplantation Center, Seoul National University Hospital, Seoul, Korea

<sup>7</sup>Department of Laboratory Medicine, Seoul National University College of Medicine, Seoul, Korea

<sup>8</sup>Department of Laboratory Medicine, Boramae Hospital, Seoul, Korea

<sup>9</sup>Seoul Metropolitan Government Public Cord Blood Bank, Seoul, Korea

**Correspondence**

Ohsang Kwon  
Email: oskwon@snu.ac.kr

**Funding information**

Korea Health Industry Development Institute (KHIDI), Grant/Award Number: HI13C1853; Seoul National University Hospital (SNUH) Research Fund, Grant/Award Number: 0320160070 (2016-1032)

Dendritic cells (DCs) are key targets for immunity and tolerance induction; they present donor antigens to recipient T cells by donor- and recipient-derived pathways. Donor-derived DCs, which are critical during the acute posttransplant period, can be depleted in graft tissue by forced migration via ultraviolet B light (UVB) irradiation. Here, we investigated the tolerogenic potential of donor-derived DC depletion through in vivo and ex vivo UVB preirradiation (UV) combined with the injection of anti-CD154 antibody (Ab) into recipients in an MHC-mismatched hair follicle (HF) allograft model in humanized mice. Surprisingly, human HF allografts achieved long-term survival with newly growing pigmented hair shafts in both Ab-treated groups (Ab-only and UV plus Ab) and in the UV-only group, whereas the control mice rejected all HF allografts with no hair regrowth. Perifollicular human CD3<sup>+</sup> T cell and MHC class II<sup>+</sup> cell infiltration was significantly diminished in the presence of UV and/or Ab treatment. HF allografts in the UV-only group showed stable maintenance of the immune privilege in the HF epithelium without evidence of antigen-specific T cell tolerance, which is likely promoted by normal HFs in vivo. This immunomodulatory strategy targeting the donor tissue exhibited novel biological relevance for clinical allogeneic transplantation without generalized immunosuppression.

**KEYWORDS**

basic (laboratory) research/science, dendritic cell, dermatology, immunosuppression/immune modulation, stem cells, tissue (nonvascularized) transplantation, tolerance, experimental, translational research/science

## 1 | INTRODUCTION

Dendritic cells (DCs) are key targets for the induction of immunity and tolerance based on their role in the process of antigen presentation for immune recognition.<sup>1,2</sup> Both donor-derived (direct pathway) and recipient-derived (indirect pathway) DCs can present donor antigens to recipient T cells. These pathways result in the expansion of recipient T cell clones restricted to either donor or recipient MHC molecules.<sup>3</sup> In particular, donor-derived “passenger” DCs are critical parts of the acute rejection mechanism that exert direct alloimmune responses of unusual strength when recognized by recipient T cells through direct pathway.<sup>3-5</sup>

Hair follicles (HFs) are dynamic structures that undergo lifelong cycles, consisting of anagen (active growth), catagen (regression), and telogen (relative rest) phases.<sup>6</sup> The generation of a new hair cycle depends on the activation of HF stem cells, which are preserved in the bulge region of the HF epithelium.<sup>7</sup> Immunologically, HFs enjoy immune privilege (IP) from the bulge to bulb, which suppresses inflammation and promotes immune tolerance.<sup>8-11</sup> HFs also play a role as portals for the entry of pre-Langerhans cells (LCs) into the epidermis.<sup>12</sup> Clinically, autologous HF transplantation is considered an effective treatment option for permanent alopecia. However, a patient with severe permanent alopecia cannot benefit from an autologous source because of the unmet shortage of donor HFs. In particular, after high-dose conditioning chemotherapy, childhood cancer survivors often have permanent chemotherapy-induced alopecia.<sup>13</sup> Although parents often wish to donate some of their hair to their children, allogeneic HF transplantation cannot be successful without generalized immunosuppression, and the associated side effects of long-term immunosuppression cannot be justified in the case of non-life-threatening conditions. Therefore, a new immunomodulatory tool is needed to enable the success of HF allografts.

Ultraviolet (UV) radiation, especially UVB (280-320 nm), is well known to suppress cellular immunity in the skin.<sup>14,15</sup> UVB phototherapy can inhibit natural killer (NK) cell activity and decrease the number of epidermal T cells and DCs in the skin.<sup>15-17</sup> Meanwhile, the anti-CD154 (CD40L) antibody (Ab) is a costimulation blocking agent involved in DC maturation and is required for T cell activation.<sup>18</sup> Sufficient DC maturation prior to antigen presentation is essential for the development of active cytotoxic T cells.<sup>19</sup> Therefore, we posited that application of UVB irradiation to graft tissue prior to transplantation would efficiently deplete donor-derived DCs and that injection of anti-CD154 Ab into recipient animals would prevent recipient-derived DCs from activating the recipient T cells (Figure S1).<sup>20</sup>

In this study, we evaluated the tolerogenic potential of UVB preirradiation combined with anti-CD154 Ab treatment in an MHC-mismatched HF allograft model in humanized mice. First, the depletion of donor-derived DCs in graft tissue was evaluated after 2 rounds of *in vivo* and *ex vivo* UVB irradiation. Then, the donor HFs were transplanted into the back skin of humanized mice with anti-CD154 Ab treatment for adjuvant blocking of recipient-derived DCs. The survival of HF allografts was evaluated by photography, histology, immunostaining, and enzyme-linked immunospot (ELISPOT)

assays until 6 months posttransplant. The results of this study provide a scientific foundation for developing a novel approach for clinical application of HF allografts to reduce the detrimental effects of generalized immunosuppression.

## 2 | MATERIALS AND METHODS

### 2.1 | UVB irradiation of *ex vivo* microdissected HFs and *in vivo* and *ex vivo* donor HFs

A UVB irradiation device containing F75/85W/UV21 fluorescent sun lamps (Philips, Eindhoven, the Netherlands) was used after measuring the UVB intensity with a UV photometer (585100; Waldmann, Villingen-Schwenningen, Germany). Then, microdissected human HFs were single irradiated with UVB at doses of 0 mJ/cm<sup>2</sup>, 50 mJ/cm<sup>2</sup>, and 150 mJ/cm<sup>2</sup> and incubated for 4 hours. For the detection of migrating donor-derived DCs, cells in the medium and dish plate were collected after trypsin treatment, incubated with anti-hCD1a Ab (M0721; Dako, Glostrup, Denmark), and followed by fluorescein isothiocyanate-labeled anti-mouse Ab (F0479, Dako). Flow cytometric analysis was performed with a FACSCalibur instrument (BD Biosciences, San Jose, CA). For the HF allografts, half of the shaved occipital scalp was irradiated with the suberythema dose (0.9 minimal erythema dose) *in vivo* 3 days before transplantation. Then, the *ex vivo* microdissected donor HFs were irradiated with an additional dose (50 mJ/cm<sup>2</sup>) 4 hours before transplantation.

### 2.2 | Generation of human hematopoietic stem cell-engrafted humanized mice

Humanized mice were generated as previously described.<sup>21</sup> A total of 68 8-week-old male NSG mice (NOD.Cg-Prkdc<sup>scid</sup>Il2rg<sup>tm1Wjl</sup>/SzJ, 005557; The Jackson Laboratory, Bar Harbor, ME) were irradiated with a 220-cGy whole-body <sup>137</sup>Cs gamma irradiator. A total of 23 fresh human umbilical cord blood packs were provided from Allcord, Seoul Metropolitan Government Public Cord Blood Bank. Umbilical cord blood packs were purified into highly enriched hCD34<sup>+</sup> hematopoietic stem cell (HSC) populations using a MicroBead Kit (130-046-703, Miltenyi Biotec, Bergisch Gladbach, Germany). Approximately 90% of the cells were hCD34<sup>+</sup> when the purity was evaluated by flow cytometric analysis. HSC populations were divided into injection units (an appropriate amount for a mouse) of between 1.5 × 10<sup>5</sup> and 2.0 × 10<sup>5</sup> cells. Then, the injection units were randomly inoculated intravenously into mice within 4 hours after gamma irradiation. The reconstitution of human immune cells was monitored at 12 and 16 weeks posttransplant. Peripheral blood samples from humanized mice were centrifuged and washed after red blood cell lysis and then incubated with the following fluorochrome-labeled monoclonal antibodies: anti-hHLA-ABC (YG13; BD Biosciences), hCD14 (MEM-18; BD Biosciences), hCD19 (HIB19; BD Biosciences), and

hCD3 (UCHT1; BD Biosciences), then evaluated by flow cytometric analysis. Lymphocytes were gated based on their forward- and side-scatter characteristics, and the positive population was quantified in hHLA-ABC<sup>+</sup> cells. All animal procedures were approved by the Institutional Animal Care and Use Committee, Seoul National University (SNU-150212-5, SNU-150212-6).

### 2.3 | Human HF transplantation

Donor HFs were harvested from the occipital scalp of healthy human volunteers and dissected to minimize the amount of connective tissue sheath remaining. Microdissected HFs were transplanted into the upper back skin of mice via follicular unit, with a goal of a total of 40 transplanted HFs. A anti-human CD154 monoclonal Ab (dose 20 mg/kg, 5C8 clone derivative; National Institutes of Health, Bethesda, MD) was injected into recipient mice intraperitoneally at -7, -3, 0, 3, 7, 12, and 17 days and then at 3, 4, 5, 6, 7, 8, 10, and 12 weeks posttransplant. The number of visible HF allografts was evaluated via biopsy at 3 days at 1, 2, and 4 weeks; and then every 4 weeks until 16 weeks posttransplant. Some HF allografts were buried and became ingrown HFs under the thin murine skin.<sup>22</sup> Therefore, an initial decrease of visible HF allografts was compensated based on the nonhumanized mice group. The original hair shafts undergo shedding out after transplantation, and new hair shafts regrow during the subsequent hair cycle.<sup>23</sup> The final number of visible HF allografts was calculated as the surviving HF allografts at all previous time points. This study was conducted according to the approved protocol by the Institutional Review Board at Seoul National University Hospital (IRB-1212-118-454).

### 2.4 | Histology, immunohistochemistry, and immunofluorescence

Immunohistochemical staining was performed using the following primary antibodies: anti-hCD3 (A0452; Dako), anti-hHLA-DP, -DQ, and -DR (MHC class II, M0775; Dako), and anti-hHLA-ABC (MHC class I, SC-25619; Santa Cruz Biotechnology, Dallas, TX). Then, the slides were treated with the SPlink HRP Broad Bulk Kit (D01-110, GBI labs, Bothell, WA). Immunofluorescence staining was performed using the following primary antibodies: anti-hCD1a (M0721; Dako), anti-hCD11c (3.9; BioLegend, San Diego, CA), anti-hHLA-DP, -DQ, and -DR (MHC class II, M0775; Dako), anti-p53 (DO7, NCL-L-p53-DO7; Novocastra, Wetzlar, Germany), and anti-K15 (LHK15; Lab Vision, Fremont, CA). Then, the slides were incubated with the Alexa-Fluor 488/594-labeled goat IgG Ab (Thermo Fisher, Waltham, MA). The nuclei were counterstained with 4',6-diamidino-2-phenylindole (Dako). For terminal deoxynucleotidyl transferase-mediated dUTP nick end-labeling (TUNEL) staining, the slides were stained using an ApopTag fluorescein in situ apoptosis detection kit (S7110; Merck Millipore, Darmstadt, Germany). Positively stained cells distributed in the HFs and at a distance of the diameter of a hair bulb from the HFs were counted as previously reported.<sup>24,25</sup> Corrected total cell

fluorescence was calculated as the integrated density (area of selected cell × mean fluorescence of background readings) using ImageJ software (National Institutes of Health).

### 2.5 | ELISPOT assay

The quantity of interferon (IFN)- $\gamma$ -secreting T cells in the spleens of humanized mice was measured using an ELISPOT kit (Mabtech, Nacka Strand, Sweden). Briefly,  $3 \times 10^5$  splenocytes from the recipient humanized mice were cultured with  $5 \times 10^4$  human PBMCs from donors for 40 hours at 37°C. As a negative control, the recipient splenocytes were left unstimulated; as a positive control, the cells were stimulated with third-party  $\gamma$ -irradiated human PBMCs. As a hCD3<sup>+</sup> T cell control, the cells were stimulated with anti-hCD3 Ab. Then, the cells were removed, and alkaline-phosphatase-conjugated Ab (1:1000) against IFN- $\gamma$  was added, followed by the addition of 100  $\mu$ L of BCIP/NBT substrate. The IFN- $\gamma$ -specific spots were counted on a computer-assisted ELISPOT Reader System (Autoimmun Diagnostika, Straßberg, Germany). The results were normalized to the hCD3<sup>+</sup> T cell control to match the number of total human T cells among the total splenocytes.

### 2.6 | Statistical analysis

Data are shown as the mean  $\pm$  standard error of the mean. All statistical analyses were performed using SPSS version 22 (IBM Corp., Armonk, NY). Student *t* test, the Mann-Whitney *U* test, the log-rank test, and 2-way analysis of variance followed by a Bonferroni post hoc test were used for determining statistical significance.

## 3 | RESULTS

### 3.1 | Donor-derived DCs are depleted by UVB preirradiation in HFs

UVB irradiation of the skin induces the depletion of epidermal DCs by their migration out of the exposed skin to the lymph nodes rather than by apoptosis.<sup>14,26,27</sup> Simultaneously, UVB is a major environmental hazard that can induce apoptosis in the HF epithelium.<sup>27,28</sup> To determine the migration-inducing but minimally toxic dose of UVB irradiation, microdissected human HFs were treated with UVB irradiation and incubated for 4 hours (Figure 1A). The dose of 50 mJ/cm<sup>2</sup> induced a reduction of CD1a<sup>+</sup> cells by about half in the isthmus and lower infundibulum of the HF epithelium (Figure 1B). Migrating CD1a<sup>+</sup> cells were detected in the medium and dish plate (Figure 1C). At a dose of 150 mJ/cm<sup>2</sup>, CD1a<sup>+</sup> cells migrated more (Figure 1B), but p53-dependent TUNEL<sup>+</sup> cells were observed in the K15<sup>+</sup> HF stem cell layer (Figure 1D), indicating UV-induced apoptosis with the coexpression of cleaved caspase-3 (Figure 1E). To obtain complete depletion, 1 round was added to the in vivo scalp 3 days before transplantation (Figure S2; 0.9 minimal erythema dose), followed by the other round to the ex vivo follicular unit

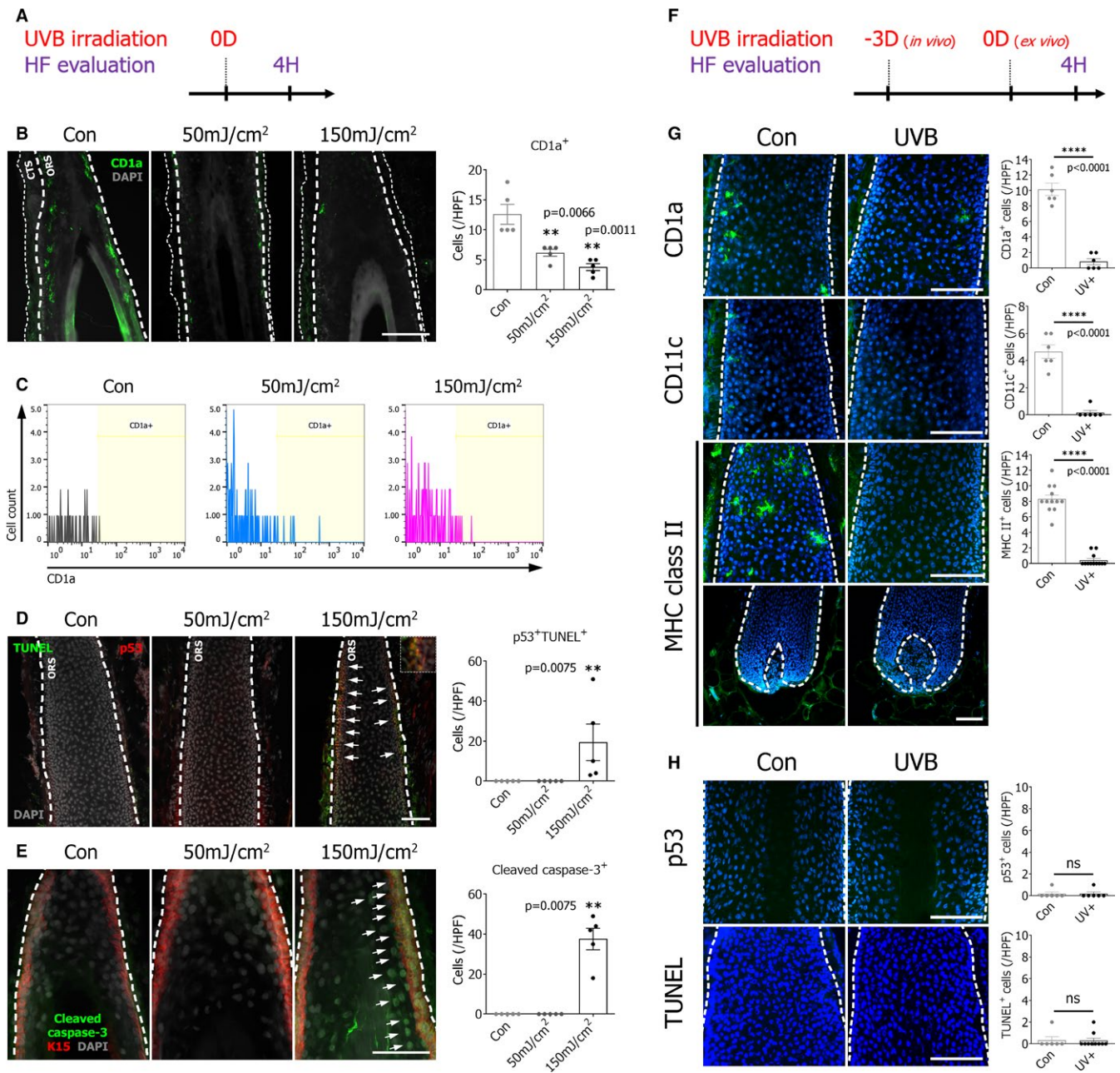


**FIGURE 1** Donor-derived DCs are depleted by UVB preirradiation in HF without apoptotic damage. **A**, Schedule of single UVB irradiation of ex vivo microdissected HF. **B**, Representative images and quantification of CD1a staining to detect donor-derived DCs in nonirradiated and UVB-irradiated HF (0 mJ/cm<sup>2</sup>, 50 mJ/cm<sup>2</sup>, and 150 mJ/cm<sup>2</sup>; n = 5 HF/group). **C**, Representative flow cytometric analysis of CD1a<sup>+</sup> cells to detect migrating DCs in the medium and dish plate of nonirradiated and UVB-irradiated HF (n = 20 HF/group). **D**, Representative images and quantification of p53 and TUNEL staining to detect UVB-induced apoptosis (white arrow; n = 5 HF/group). **E**, Representative images and quantification of cleaved caspase-3 staining to detect apoptotic cell death in the K15<sup>+</sup> HF stem cell layer (white arrow; n = 5 HF/group). **F**, Schedule of 2 separate rounds of in vivo and ex vivo UVB irradiation of donor HF. **G**, Representative images of CD1a, CD11c, and MHC class II staining to detect donor-derived DCs in nonirradiated and UVB-irradiated donor HF (n = 6, 6, and 12 HF/group). **H**, Representative images of p53 and TUNEL staining to detect UVB-induced apoptosis (n = 6 and 10 HF/group; immunofluorescence; scale bar = 100 μm). \*\*P < .01 (Mann-Whitney U test); \*\*\*\*P < .0001 (unpaired t test). Con, control; CTS, connective tissue sheath; D, day; DAPI, 4',6-diamidino-2-phenylindole; DCs, dendritic cells; H, hour; HF, hair follicle; HPF, high-power field; K, keratin; ORS, outer root sheath; ns, not significant; TUNEL, terminal deoxynucleotidyl transferase-mediated dUTP nick end-labeling; UVB, ultraviolet B light

(50 mJ/cm<sup>2</sup>) 4 hours before transplantation (Figure 1F).<sup>29,30</sup> At the time point immediately before transplantation, donor-derived DCs (CD1a<sup>+</sup>, CD11c<sup>+</sup>, and MHC class II<sup>+</sup>) disappeared almost completely

in UVB-irradiated HF (Figure 1G), and DCs were rarely seen in the bulb area.<sup>31</sup> There was no evidence of UV-induced apoptosis (p53<sup>+</sup> or TUNEL<sup>+</sup>) in UVB-irradiated HF (Figure 1H).

### 3.2 | UVB preirradiation alone enables long-term survival of HF allografts

To evaluate the acceptability of HF allografts in humans, humanized mice were generated with hCD34<sup>+</sup> HSC engraftment,<sup>32</sup> which is an optimal model because human DCs and alloreactive T cells are generated (Figure S3 and Table S1).<sup>21,33,34</sup> In total, 24 humanized mice were enrolled as recipients (HM groups) according to the criteria of having >1% hHLA-ABC<sup>+</sup>hCD3<sup>+</sup> T cells present in the peripheral blood (mean 3.18 ± 0.49%; Figure S3D). Nonhumanized mice were included to eliminate bystander bias from the xenogeneic immune response to human tissue. Each mouse received human HF allografts in the upper back skin (Figure 2A; total 1104 HF allografts, mean 36.8 ± 0.86 HF/mouse).

Intriguingly, the surviving HF allografts were maintained and eventually achieved long-term survival in all treated recipients (HM UV+Ab, HM Ab, and HM UV) in addition to in the nonhumanized recipients (NSG Con). The surviving HF allografts showed newly growing black-pigmented hair shafts (Figures 2B,C, S4, and S5). However, in the control mice (HM Con), the HF allografts rapidly diminished within 4 weeks, and no hair regrowth or ingrown HF were observed. By relative analysis to the NSG Con group, approximately half of the HF allografts achieved long-term survival in the HM UV+Ab, HM Ab, and HM UV groups (Figure 2D). Based on the existence of ingrown HF when the mice were euthanized, the actual survival rate is expected to be higher than indicated by the visible HF allografts (Figure 2E). Histological examination showed that the outer root sheath (ORS) was maintained with an orderly structure in the surviving HF allografts (Figure 3). However, in the HM Con group, the ORS underwent destruction by perifollicular inflammation and was replaced with large amounts of inflammatory granuloma. Taken together, we concluded that the combined and single treatments with UVB preirradiation and/or anti-CD154 Ab achieved long-term survival of the HF allografts.

### 3.3 | Inflammatory cell infiltration is diminished under UV and/or Ab treatment

To evaluate the immunomodulatory mechanism, perifollicular human CD3<sup>+</sup> T cells and MHC class II<sup>+</sup> cells were assessed. In the dermis, MHC class II<sup>+</sup> cells represent professional antigen presenting cells (DCs, monocytes, and macrophages) and non-APC subsets (activated T cells).<sup>35</sup> The timing and amount of hCD3<sup>+</sup> T cell infiltration were significantly delayed and reduced (Figures 4A and S6), and the amount of hMHC class II<sup>+</sup> cell infiltration was reduced (Figures 4B and S7) in the HM UV+Ab, HM Ab, and HM UV groups. However, T cells and macrophages had already infiltrated at week 1 and persisted as an inflammatory aggregation in the HM Con group. These results demonstrated that UVB preirradiation significantly suppressed alloreactive T cell and macrophage infiltration, regardless of whether there was a concomitant anti-CD154 Ab treatment.

When the humanized mice were euthanized at 24 weeks post-transplant, hHLA-ABC<sup>+</sup>hCD3<sup>+</sup> T cells were still observed in the total splenocytes (Figure 5A; mean 7.90 ± 0.67%). To assess whether the recipient mice developed antigen-specific T cell tolerance against donor HF, the total splenocytes were left unstimulated, stimulated with donor PBMCs, or stimulated with third-party  $\gamma$ -irradiated human PBMCs, followed by ELISPOT assays (Figures 5B and S8). Interestingly, the IFN- $\gamma$ -secreting T cells against donor antigens were not suppressed in the UV-only group (HM UV) compared to the Ab-treated groups (HM UV+Ab and HM Ab). Therefore, we speculated that antigen-specific T cell tolerance was not the major mechanism underlying the long-term survival of HF allografts in the UV-only group.

### 3.4 | IP is maintained with intact HF stem cells in surviving HF allografts

HF is a unique site of IP in the skin, characterized by an absence of MHC class I molecules and the expression of potent immunosuppressants.<sup>36,37</sup> Specifically, IP in the bulge region restricts autoantigen presentation and protects HF stem cells against cytotoxic T cell attack.<sup>38,39</sup> To examine the possibility that IP contributed to the long-term survival of HF allografts in the UV-only group, IP status was evaluated in the bulge and bulb epithelium. In the control mice, the ORS of the HF remnants showed strong MHC class I expression in the bulge (Figures 6A and S9) and bulb (Figure 6B) at 4 weeks posttransplant, indicating IP collapse as observed in permanent hair loss associated with lichen planopilaris.<sup>11,39,40</sup> Moreover, the K15<sup>+</sup> HF stem cell layer was lost in the MHC class I<sup>+</sup> HF remnant. In contrast, the ORS in surviving HF allografts maintained downregulated expression of MHC class I along with an intact K15<sup>+</sup> HF stem cell layer, demonstrating an intact IP in the MHC-mismatched recipients. Then, the DC repopulation was investigated for human MHC class II<sup>+</sup> cells exhibiting a DC morphology located inside HF allografts.<sup>12</sup> At day 3 posttransplant, there were no detectable DCs in all groups; however, the presence of DCs was observed at week 4 in surviving HF allografts (Figures 6C and S10). In the control mice, few MHC class II<sup>+</sup> cells were detected inside the HF remnant but showed a T cell morphology rather than that of DCs.

## 4 | DISCUSSION

The alloreactive T cell response represents the rate-limiting step involved in allograft rejection, which manifests as indefinite allograft acceptance in T cell-receptor-deficient animal models.<sup>3</sup> We previously demonstrated that the major contributor to the rejection of HF allografts is cytotoxic T cells in the skin of nonhuman primates.<sup>25</sup> Therefore, the antigen presentation process is critical for the induction of T cell-mediated rejection of HF allografts. Donor-derived DCs can effectively activate donor MHC-restricted recipient T cells, which are the major players capable of a direct interaction with target cells in a donor MHC-dependent manner, representing the driving



**B**

Xenogeneic	+		+	+	+	+
Allogeneic			+	+	+	+
UV			+			+
Ab			+	+		

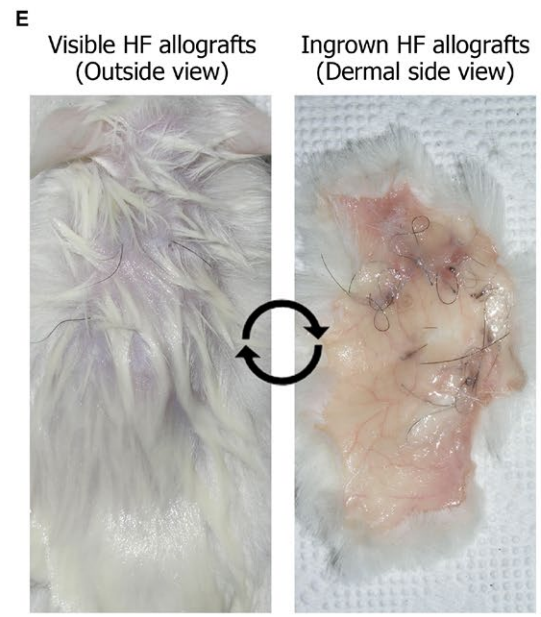
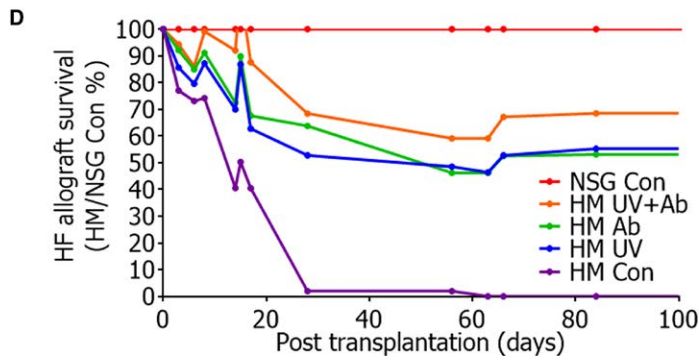
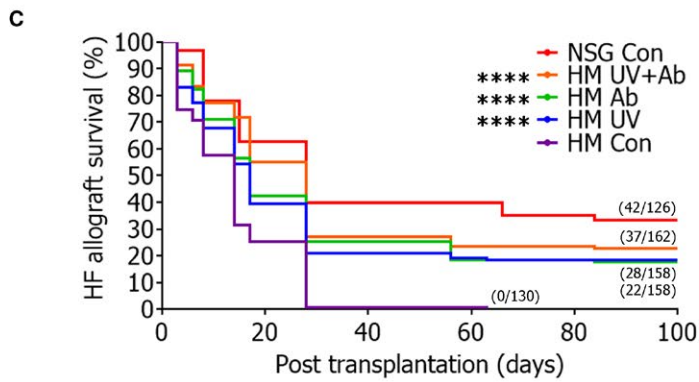
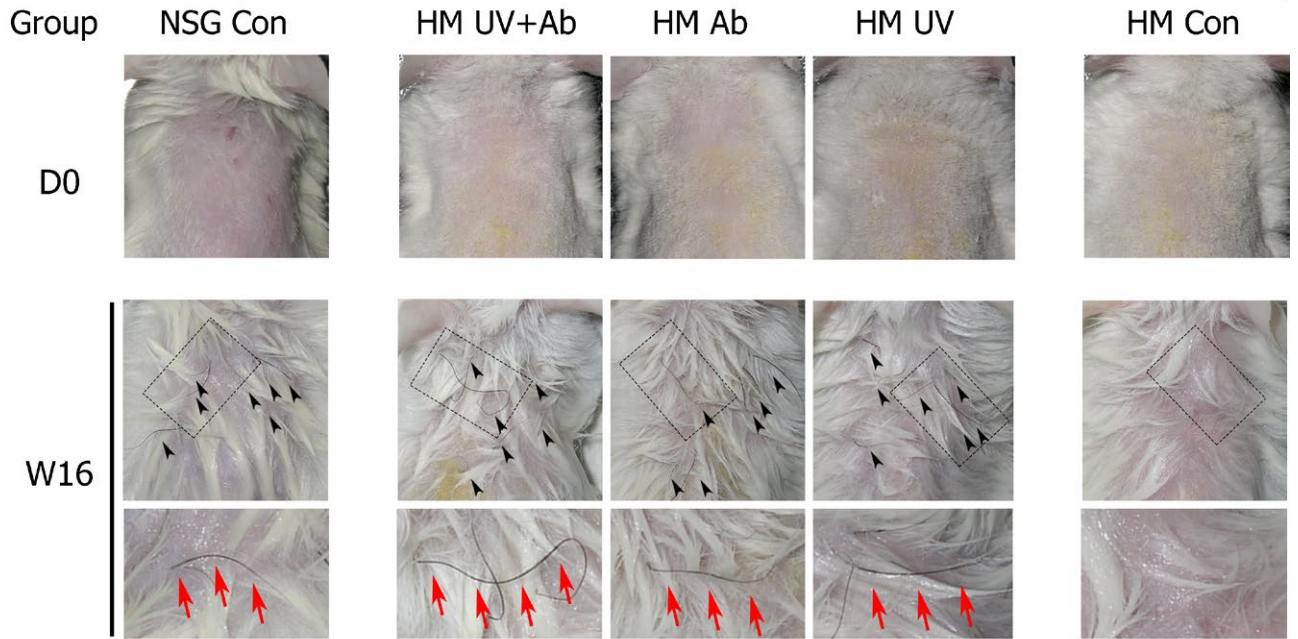


**FIGURE 2** Long-term survival of HF allografts after UVB preirradiation and/or anti-CD154 Ab treatment. A, Schedule for allogeneic HF transplantation. B, Summary of experimental groups (n = 6 mice/group). Nonhumanized mice (NSG Con). Humanized mice were divided into the following 4 groups: UVB preirradiation plus anti-CD154 Ab (HM UV+Ab), anti-CD154 Ab only (HM Ab), UVB preirradiation only (HM UV), and no treatment (HM Con). Representative photographs at 0 and 16 weeks posttransplant. Long-term survival of HF allografts (black arrowheads) was achieved, as indicated by newly growing black-pigmented hair shafts (red arrows) in the NSG Con, HM UV+Ab, HM Ab, and HM UV groups; whereas no hair regrowth or ingrown HFs were observed in the HM Con group. C, Survival curve of HF allografts (number of surviving/total HF allografts, 6 mice/group). D, Relative survival curve of HF allografts in humanized mice (HM groups) to nonhumanized mice (NSG group). E, In the dermal side view, ingrown HFs with growing hair shafts were observed in the NSG Con, HM UV+Ab, HM Ab, and HM UV groups when the recipient mice were euthanized. \*\*\*\*P < .0001 vs HM Con (log-rank test). Ab, anti-CD154 antibody; D, day; HF, hair follicle; HM, humanized mouse; UVB, ultraviolet B light; W, week

force behind acute graft rejection.<sup>3,41</sup> In this study, the human T cells that emerged in the peripheral blood of mice would be mouse MHC-restricted by thymic education in the vestigial mouse thymus. Nevertheless, the recipient T cells are capable of retaining immunoreactivity to allogeneic human MHC-peptide complexes, which is the same situation as direct alloantigen recognition explained by significant T cell receptor cross-reactivity.<sup>34</sup> This model is still satisfactory for the purpose of assessing an approach for preventing the activation of recipient T cells by a very simple and noninvasive method, namely, inducing the depletion of donor-derived DCs by UVB preirradiation.

The HF is recognized for its IP, which is similar to that of the brain, cornea, and the anterior chamber of the eye.<sup>42</sup> IP reflects the ability

of these tissue environments to avoid allograft rejection by the host immune system.<sup>43,44</sup> Despite the presence of MHC class I<sup>-</sup> cells, there is no evidence of NK cell or cytotoxic T cell attack in normal HF epithelium.<sup>45</sup> This absence of NK cell-mediated injury results from the effects associated with multiple inhibitory cytokines, including transforming growth factor- $\beta$ 2 and macrophage migration inhibitory factor.<sup>11,24,39,45</sup> Human anagen HFs maintain their IP, reducing the opportunity for NK cell activation, thereby escaping the induction of autoimmune disorders such as lichen planopilaris.<sup>8,37,39,44</sup> Under autoimmune conditions, INF- $\gamma$  induces IP collapse in the HF by promoting elevated MHC class I expression, resulting in permanent loss of HF stem cells.<sup>24,39,40</sup>

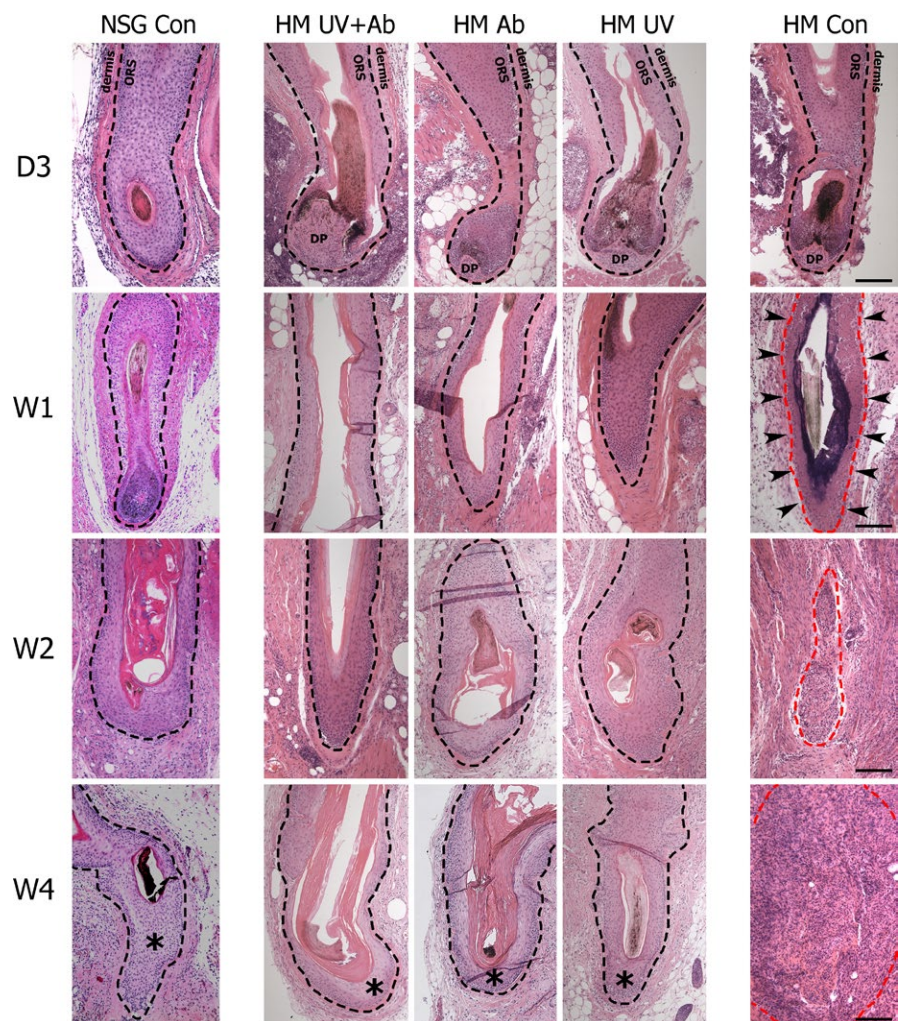


**FIGURE 3** UVB preirradiation alone achieved long-term survival of HF allografts. Representative images at 3 days and at 1, 2, and 4 weeks posttransplant. The ORS was maintained with an orderly structure (black dotted line) and was intact at 4 weeks posttransplant (asterisk) in the surviving HF allografts. However, in the HM Con group, ORS underwent destruction by perifollicular inflammation (black arrowheads) and was replaced with inflammatory granuloma (red dotted line); hematoxylin and eosin staining; n = 6 HFs/time point, 6 mice/group; scale bar = 100  $\mu$ m). Ab, anti-CD154 Ab; D, day; HF, hair follicle; HM, humanized mouse; DP, dermal papilla; ORS, outer root sheath; UVB, ultraviolet B light; W, week

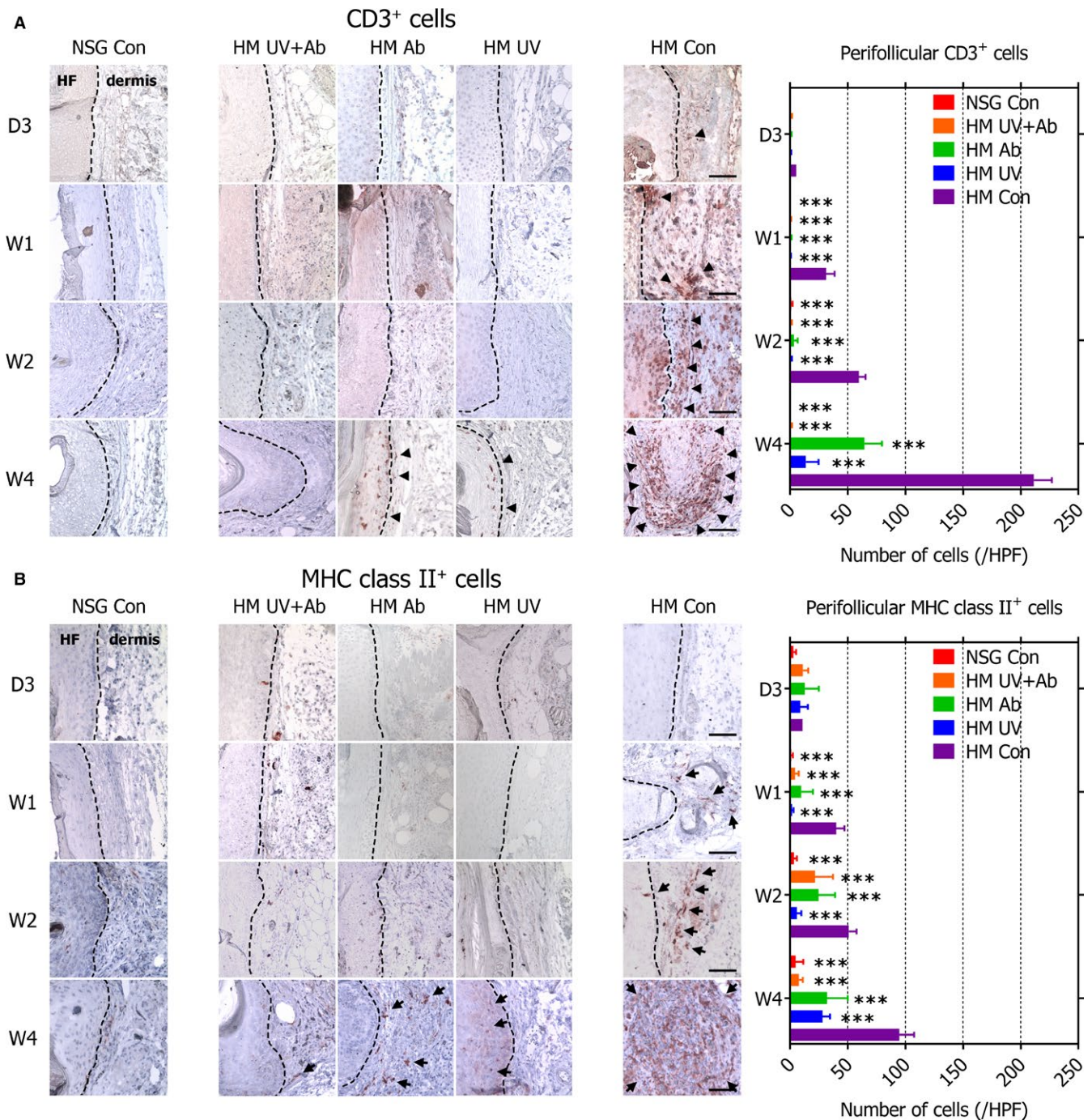


**FIGURE 4** Perifollicular CD3<sup>+</sup> T cell and MHC class II<sup>+</sup> cell infiltration was diminished under UVB preirradiation and/or anti-CD154 Ab treatment. Representative images and quantification of perifollicular human (A) CD3<sup>+</sup> T cells (arrowhead) and (B) MHC class II<sup>+</sup> cells (arrow) at 3 days and at 1, 2, and 4 weeks posttransplant (immunoperoxidase,  $n = 6$  HF/time point, 6 mice/group; scale bar = 50  $\mu\text{m}$ ). \*\*\* $P < .001$  vs HM Con (2-way analysis of variance, Bonferroni post hoc test). Ab, anti-CD154 Ab; D, day; HM, humanized mouse; HPF, high-power field; UVB, ultraviolet B light; W, week

The most striking finding of the present study was that the UV-only treated HF allografts survived for a long time in MHC-mismatched recipients. A previous study showed that the depletion of donor-derived LCs by UV radiation promoted graft survival in a corneal allograft model.<sup>46</sup> We also observed long-term survival by forcing donor-derived DCs to migrate out of graft tissue, which consequently eliminated the possibility of direct alloantigen presentation.

In this context, IP is supposed to play a key role in the long-term survival of HF allografts, despite the absence of recipient MHC class I molecules in the MHC-mismatched recipient.<sup>47</sup> This finding is reminiscent of normal HF, which are not rejected in the absence of MHC class I molecules. Surveillance by recipient-derived DCs via the indirect pathway might be evaded due to the immunosuppressive characteristics of IP. Taken together, our findings indicated that the

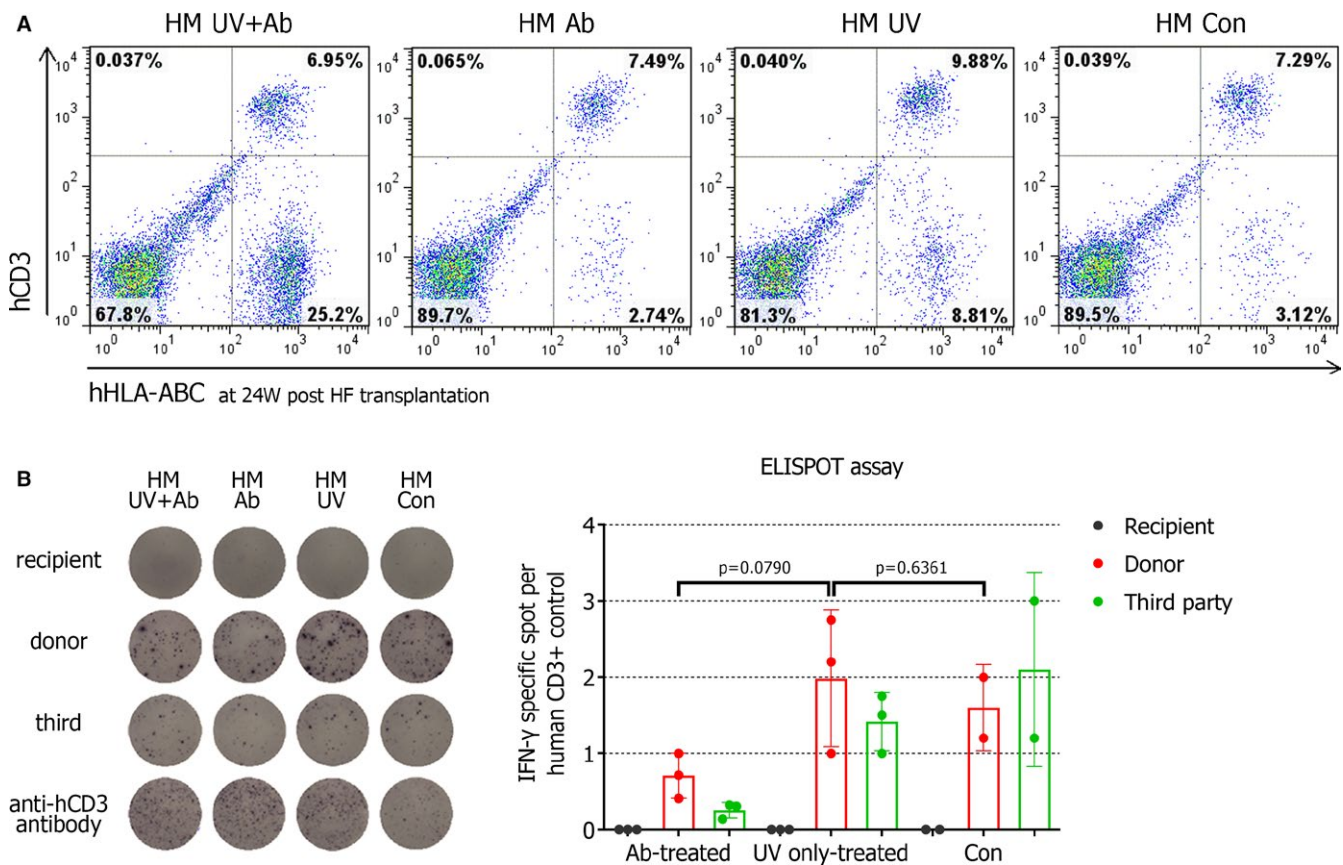


**FIGURE 5** UVB preirradiation alone did not induce antigen-specific T cell tolerance. A, Representative flow cytometry plots of hHLA-ABC<sup>+</sup>hCD3<sup>+</sup> T cells among the total splenocytes from humanized mice when they were euthanized at 24 weeks posttransplant. B, Summarized data from the ELISPOT assays evaluating IFN- $\gamma$ -secreting T cells that were left unstimulated (recipient), stimulated with donor PBMCs (donor) or third-party  $\gamma$ -irradiated human PBMCs (third party), normalized to human CD3<sup>+</sup> T cell control (n = 2-3 mice/group). Ab, anti-CD154 Ab; HF, hair follicle; HM, humanized mouse; IFN- $\gamma$ , interferon- $\gamma$ ; PBMCs, peripheral blood mononuclear cells; UVB, ultraviolet B light

depletion of donor-derived DCs prior to transplantation is sufficient to ensure the survival of IP organs by decreasing alloreactive T cell infiltration, which is likely promoted by normal HFs in vivo.

The CD40-CD154 pathway acts on both APCs and T cells in a bi-directional fashion, and this costimulatory pathway plays a central role in DC activation and maturation.<sup>48-50</sup> The cross-linking of CD40 on DCs by CD154 on activated CD4<sup>+</sup> T cells leads to the licensing of the APCs, the upregulation of costimulatory molecules, and the production of proinflammatory cytokines.<sup>51,52</sup> The interaction of CD154 on activated CD4<sup>+</sup> T cells and CD40 on CD8<sup>+</sup> T cells plays a critical role in generating effective cytotoxic T cell responses.<sup>53</sup> However, antigen presentation by semimature or immature DCs results in T cell tolerance due to a failure to provide sufficient costimulatory signals.<sup>19,54</sup> Therefore, a dual-blocking strategy is relevant involving donor- and recipient-derived DCs through both UVB preirradiation and anti-CD154 Ab in the alloantigen presentation process.

In the skin, LCs self-renew and are not replaced by circulating precursors at a steady state,<sup>55</sup> as shown in the skin xenograft model in which donor-derived DCs persisted for more than 9 weeks.<sup>56</sup> Following UV irradiation, pre-LCs arose from monomyeloid precursors and rapidly repopulated into the epidermis via HFs after 2-3 weeks.<sup>12</sup> In the present study, we could easily detect human MHC class II<sup>+</sup> DCs

in the surviving HF allografts, including those in the nonhumanized mice that did not harbor a humanized immune system. Therefore, we suggested that the repopulated DCs primarily represented surviving donor passengers that had previously migrated out of the site, as well as host-derived DCs from the humanized immune system based on the UV-treated groups.

Previously, we demonstrated that the anti-ICAM-1 Ab combined with short-term rapamycin treatment enhances HF allograft survival in a nonhuman primate model.<sup>25</sup> This attempt efficiently suppressed the alloreactive T cell response but only targeted the recipient hosts, resulting in a lack of long-term survival of HF allografts. The tissue at the interface between the body and environment already contains many resident immune cells, which are unlikely to be found in the visceral organs.<sup>57,58</sup> However, in this type of tissue, there is the potential for immunomodulation, such as UVB preirradiation, to be easily applicable. In the present study, the visible survival of HF allografts may not be sufficient to translate directly to clinical application because of the undesirable circumstances caused by the limitations of the mechanical xenograft model. Nevertheless, the achievement of long-term survival has clinical relevance for preventing allograft rejection by targeting the donor tissue, moving 1 step closer toward allogeneic transplantation without generalized immunosuppression.

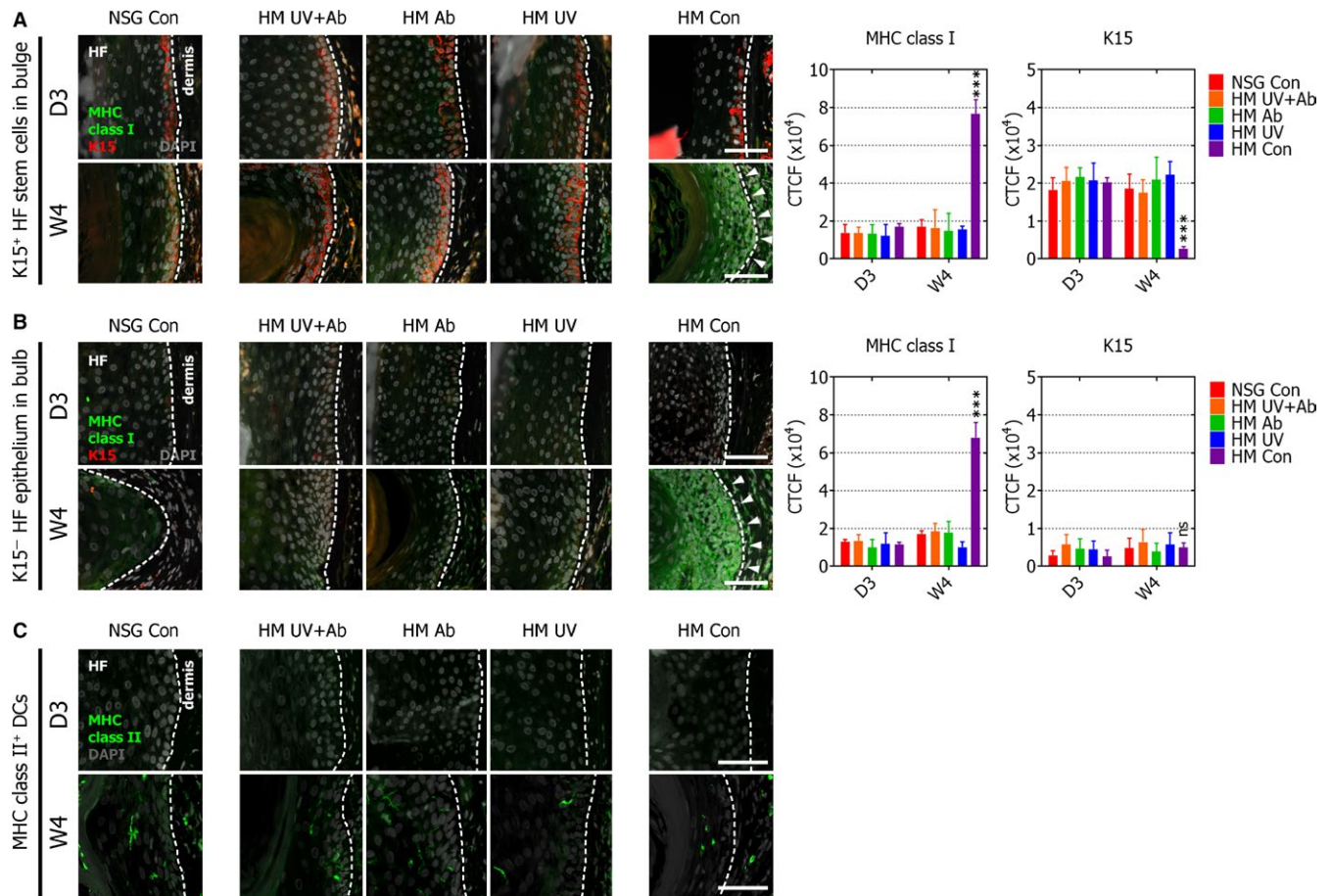


**FIGURE 6** IP was maintained with intact HF stem cells in the surviving HF allografts exhibiting DC repopulation. Representative images and quantification of human MHC class I and K15 expression in the (A) bulge and (B) bulb of the HF epithelium at 3 days and 4 weeks posttransplant. The ORS of HF remnants showed strong MHC class I expression with loss of the K15<sup>+</sup> HF stem cell layer in the control mice (HM Con, white arrowhead; n = 4 HF/time point, 6 mice/group). C, Representative images of human MHC class II<sup>+</sup> DCs inside HF allografts at 3 days and 4 weeks posttransplant (immunofluorescence; scale bar = 50  $\mu$ m). \*\*\* $P$  < .001 (2-way analysis of variance, Bonferroni post hoc test). Ab, anti-CD154 Ab; CTCF, corrected total cell fluorescence; D, day; DCs, dendritic cells; HF, hair follicle; HM, humanized mouse; IP, immune privilege; K, keratin; ns, not significant; ORS, outer root sheath; UV, ultraviolet light; W, week

## ACKNOWLEDGMENTS

We greatly appreciate Professor George Cotsarelis (Perelman School of Medicine, University of Pennsylvania, Philadelphia, PA) for valuable comments and discussions. This research was supported by a grant from the Korea Health Technology R&D Project through the Korea Health Industry Development Institute (KHIDI) funded by the Ministry of Health & Welfare, Republic of Korea (No. HI13C1853) and by a grant from the Seoul National University Hospital (SNUH) Research Fund (No. 0320160070 [2016-1032]). Umbilical cord blood was provided by Allcord, Seoul Metropolitan Government Public Cord Blood Bank, SMG-SNU Boramae Hospital.

## DISCLOSURE

The authors of this manuscript have no conflicts of interest to disclose as described by the *American Journal of Transplantation*.

## ORCID

Jin Yong Kim  <https://orcid.org/0000-0002-2069-4009>

Ohsang Kwon  <https://orcid.org/0000-0003-0464-5124>

## REFERENCES

- Steinman RM, Hawiger D, Nussenzweig MC. Tolerogenic dendritic cells. *Annu Rev Immunol*. 2003;21:685-711.
- Jung KC, Park CG, Jeon YK, et al. In situ induction of dendritic cell-based T cell tolerance in humanized mice and nonhuman primates. *J Exp Med*. 2011;208(12):2477-2488.
- Lin CM, Gill RG. Direct and indirect allograft recognition: pathways dictating graft rejection mechanisms. *Curr Opin Organ Transplant*. 2016;21(1):40-44.
- Veerapathran A, Pidala J, Beato F, et al. Ex vivo expansion of human tregs specific for alloantigens presented directly or indirectly. *Blood*. 2011;118(20):5671-5680.
- Bain B, Vas MR, Lowenstein L. The development of large immature mononuclear cells in mixed leukocyte cultures. *Blood*. 1964;23:108-116.

6. Schneider MR, Schmidt-Ullrich R, Paus R. The hair follicle as a dynamic miniorgan. *Curr Biol*. 2009;19(3):R132-R142.
7. Hsu YC, Pasolli HA, Fuchs E. Dynamics between stem cells, niche, and progeny in the hair follicle. *Cell*. 2011;144(1):92-105.
8. Paus R, Ito N, Takigawa M, et al. The hair follicle and immune privilege. *J Invest Dermatol*. 2003;8(2):188-194.
9. Westgate GE, Craggs RI, Gibson WT. Immune privilege in hair growth. *J Invest Dermatol*. 1991;97(3):417-420.
10. Paus R, Bulfone-Paus S, Bertolini M. Hair follicle immune privilege revisited: the key to alopecia areata management. *J Invest Dermatol*. 2018;19(1):S12-S17.
11. Meyer KC, Klatter JE, Dinh HV, et al. Evidence that the bulge region is a site of relative immune privilege in human hair follicles. *Br J Dermatol*. 2008;159(5):1077-1085.
12. Nagao K, Kobayashi T, Moro K, et al. Stress-induced production of chemokines by hair follicles regulates the trafficking of dendritic cells in skin. *Nat Immunol*. 2012;13(8):744-752.
13. Choi M, Kim MS, Park SY, et al. Clinical characteristics of chemotherapy-induced alopecia in childhood. *J Am Acad Dermatol*. 2014;70(3):499-505.
14. Kolgen W, Both H, van Weelden H, et al. Epidermal Langerhans cell depletion after artificial ultraviolet B irradiation of human skin in vivo: apoptosis versus migration. *J Invest Dermatol*. 2002;118(5):812-817.
15. Duthie MS, Kimber I, Norval M. The effects of ultraviolet radiation on the human immune system. *Br J Dermatol*. 1999;140(6):995-1009.
16. Racz E, Prens EP, Kurek D, et al. Effective treatment of psoriasis with narrow-band UVB phototherapy is linked to suppression of the IFN and TH17 pathways. *J Invest Dermatol*. 2011;131(7):1547-1558.
17. Krueger JG, Wolfe JT, Nabeya RT, et al. Successful ultraviolet-B treatment of psoriasis is accompanied by a reversal of keratinocyte pathology and by selective depletion of intraepidermal T-cells. *J Exp Med*. 1995;182(6):2057-2068.
18. Larsen CP, Knechtle SJ, Adams A, et al. A new look at blockade of T-cell costimulation: a therapeutic strategy for long-term maintenance immunosuppression. *Am J Transplant*. 2006;6(5 Pt 1):876-883.
19. Fujii S, Liu K, Smith C, et al. The linkage of innate to adaptive immunity via maturing dendritic cells in vivo requires CD40 ligation in addition to antigen presentation and CD80/86 costimulation. *J Exp Med*. 2004;199(12):1607-1618.
20. Zhai Y, Meng L, Gao F, et al. Allograft rejection by primed/memory CD8<sup>+</sup> T cells is CD154 blockade resistant: therapeutic implications for sensitized transplant recipients. *J Immunol*. 2002;169(8):4667-4673.
21. Pearson T, Greiner DL, Shultz LD. Creation of "humanized" mice to study human immunity. *Curr Protoc Immunol*. 2008;15:15-21.
22. Asgari AZ, Rufaut NW, Morrison WA, et al. Hair transplantation in mice: challenges and solutions. *Wound Repair Regen*. 2016;24(4):679-685.
23. Yoon JS, Choi M, Shin CY, et al. Development of a model for chemotherapy-induced alopecia: profiling of histological changes in human hair follicles after chemotherapy. *J Invest Dermatol*. 2016;136(3):584-592.
24. Ito T, Ito N, Saatoff M, et al. Maintenance of hair follicle immune privilege is linked to prevention of NK cell attack. *J Invest Dermatol*. 2008;128(5):1196-1206.
25. Kim JY, Yoon JS, Kang BM, et al. Allogeneic hair transplantation with enhanced survival by anti-ICAM-1 antibody with short-term rapamycin treatment in nonhuman primates. *J Invest Dermatol*. 2017;137(2):515-518.
26. Taguchi K, Fukunaga A, Ogura K, et al. The role of epidermal Langerhans cells in NB-UVB-induced immunosuppression. *Kobe J Med Sci*. 2013;59(1):E1-E9.
27. Braun S, Krampert M, Bodo E, et al. Keratinocyte growth factor protects epidermis and hair follicles from cell death induced by UV irradiation, chemotherapeutic or cytotoxic agents. *J Cell Sci*. 2006;119(Pt 23):4841-4849.
28. Lu Z, Fischer TW, Hasse S, et al. Profiling the response of human hair follicles to ultraviolet radiation. *J Invest Dermatol*. 2009;129(7):1790-1804.
29. Okamoto H, Mizuno K, Itoh T, et al. Evaluation of apoptotic cells induced by ultraviolet light B radiation in epidermal sheets stained by the TUNEL technique. *J Invest Dermatol*. 1999;113(5):802-807.
30. Schwarz T. Biological effects of UV radiation on keratinocytes and Langerhans cells. *Exp Dermatol*. 2005;14(10):788-789.
31. Christoph T, Muller-Rover S, Audring H, et al. The human hair follicle immune system: cellular composition and immune privilege. *Br J Dermatol*. 2000;142(5):862-873.
32. Ito M, Hiramatsu H, Kobayashi K, et al. NOD/SCID/gamma(c)(null) mouse: an excellent recipient mouse model for engraftment of human cells. *Blood*. 2002;100(9):3175-3182.
33. Shultz LD, Ishikawa F, Greiner DL. Humanized mice in translational biomedical research. *Nat Rev Immunol*. 2007;7(2):118-130.
34. Yahata T, Ando K, Nakamura Y, et al. Functional human T lymphocyte development from cord blood CD34<sup>+</sup> cells in nonobese diabetic/SHI-SCID, IL-2 receptor gamma null mice. *J Immunol*. 2002;169(1):204-209.
35. Angel CE, George E, Ostrovsky LL, et al. Comprehensive analysis of MHC-II expression in healthy human skin. *Immunol Cell Biol*. 2007;85(5):363-369.
36. Paus R, Christoph T, Muller-Rover S. Immunology of the hair follicle: a short journey into terra incognita. *J Invest Dermatol*. 1999;4(3):226-234.
37. Gilhar A, Etzioni A, Paus R. Alopecia areata. *N Engl J Med*. 2012;366(16):1515-1525.
38. Ito T, Ito N, Bettermann A, et al. Collapse and restoration of MHC class-I-dependent immune privilege: exploiting the human hair follicle as a model. *Am J Pathol*. 2004;164(2):623-634.
39. Harries MJ, Meyer K, Chaudhry I, et al. Lichen planopilaris is characterized by immune privilege collapse of the hair follicle's epithelial stem cell niche. *J Pathol*. 2013;231(2):236-247.
40. Imanishi H, Ansell DM, Cheret J, et al. Epithelial-to-mesenchymal stem cell transition in a human organ: lessons from lichen planopilaris. *J Invest Dermatol*. 2018;138(3):511-519.
41. Benichou G, Thomson AW. Direct versus indirect allorecognition pathways: on the right track. *Am J Transplant*. 2009;9(4):655-656.
42. Head JR, Billingham RE. Immunologically privileged sites in transplantation immunology and oncology. *Perspect Biol Med*. 1985;29(1):115-131.
43. Streilein JW. Immune privilege as the result of local tissue barriers and immunosuppressive microenvironments. *Curr Opin Immunol*. 1993;5(3):428-432.
44. Boehm T. Quality control in self/nonself discrimination. *Cell*. 2006;125(5):845-858.
45. Niederkorn JY. Mechanisms of immune privilege in the eye and hair follicle. *J Invest Dermatol*. 2003;8(2):168-172.
46. He YG, Niederkorn JY. Depletion of donor-derived Langerhans cells promotes corneal allograft survival. *Cornea*. 1996;15(1):82-89.
47. Reynolds AJ, Lawrence C, Cserhalmi-Friedman PB, et al. Trans-gender induction of hair follicles. *Nature*. 1999;402(6757):33-34.
48. Alaaeddine N, Hassan GS, Yacoub D, et al. CD154: an immunoinflammatory mediator in systemic lupus erythematosus and rheumatoid arthritis. *Clin Dev Immunol*. 2012;2012:490148.
49. Blair PJ, Riley JL, Harlan DM, et al. CD40 ligand (CD154) triggers a short-term CD4(+) T cell activation response that results in secretion of immunomodulatory cytokines and apoptosis. *J Exp Med*. 2000;191(4):651-660.
50. Hong J, Yeom HJ, Lee E, et al. Islet allograft rejection in sensitized mice is refractory to control by combination therapy of immunomodulating agents. *Transpl Immunol*. 2013;28(2-3):86-92.

51. Caux C, Massacrier C, Vanbervliet B, et al. Activation of human dendritic cells through CD40 cross-linking. *J Exp Med*. 1994;180(4):1263-1272.
52. Cella M, Scheidegger D, Palmer-Lehmann K, et al. Ligation of CD40 on dendritic cells triggers production of high levels of interleukin-12 and enhances T cell stimulatory capacity: T-T help via APC activation. *J Exp Med*. 1996;184(2):747-752.
53. Liu DY, Ferrer IR, Konomos M, et al. Inhibition of CD8(+) T Cell-derived CD40 signals is necessary but not sufficient for FOXP3(+) induced regulatory T Cell generation in vivo. *J Immunol*. 2013;191(4):1957-1964.
54. Shortman K, Naik SH. Steady-state and inflammatory dendritic-cell development. *Nat Rev Immunol*. 2007;7(1):19-30.
55. Merad M, Manz MG, Karsunky H, et al. Langerhans cells renew in the skin throughout life under steady-state conditions. *Nat Immunol*. 2002;3(12):1135-1141.
56. Krueger GG, Daynes RA, Emam M. Biology of langerhans cells - selective migration of langerhans cells into allogeneic and xenogeneic grafts on nude-mice. *Proc Natl Acad Sci USA*. 1983;80(6):1650-1654.
57. Abtin A, Jain R, Mitchell AJ, et al. Perivascular macrophages mediate neutrophil recruitment during bacterial skin infection. *Nat Immunol*. 2014;15(1):45-53.
58. Adachi T, Kobayashi T, Sugihara E, et al. Hair follicle-derived IL-7 and IL-15 mediate skin-resident memory T cell homeostasis and lymphoma. *Nat Med*. 2015;21(11):1272-1279.

## SUPPORTING INFORMATION

Additional supporting information may be found online in the Supporting Information section at the end of the article.

**How to cite this article:** Kim JY, Kang BM, Lee JS, et al. UVB-induced depletion of donor-derived dendritic cells prevents allograft rejection of immune-privileged hair follicles in humanized mice. *Am J Transplant*. 2018;00:1-12. <https://doi.org/10.1111/ajt.15207>